Research Article

INTERNATIONAL JOURNAL OF ADVANCED ROBOTIC SYSTEMS

International Journal of Advanced Robotic Systems
May-June 2017: 1–13

DOI: 10.1177/1729881417703568
journals.sagepub.com/home/arx
SAGE

Sliding mode control design of a ship steering autopilot with input saturation

Muhammad Ejaz and Mou Chen

Abstract

In this article, a sliding mode control scheme for the autopilot system of a ship is presented, which also incorporates actuator saturation. Under the designed controller, the actuator doesn't enter its saturation mode. Meanwhile, the stability of the closed-loop system can be guaranteed for the ship with input saturation. Fuzzy logic is used to handle gain to avoid the chattering effect, and it is compared with saturation function. The control system for the mathematical model of a scale replica of an "Esso Osaka" tanker is simulated in time domain for the effectiveness of the controller. The simulation results show that the proposed controller is more efficient as compared to the traditional and saturation function methods.

Keywords

Sliding mode control, saturation, surface vessels, autopilot systems, chattering, fuzzy logic

Date received: 16 May 2016; accepted: 27 February 2017

Topic: Robot Manipulation and Control
Topic Editor: Andrey V. Savkin
Associate Editor: Istvan Harmati

Introduction

Water being the most abundant substance at the surface of the earth makes about 1.4 billion cubic kilometers (326 million cubic miles) in the form of oceans, lakes, streams, glaciers, and groundwaters.[1] Therefore, the need for surface and subsurface vessels due to a variety of marine and offshore applications is increasing with time. These applications are related to transportation, fishing, entertainment, public safety, and warfare. In order to efficiently complete various tasks, an increment in demand of autonomous marine vessels is observed, which has opened a new door in the field of automatic control. An autopilot control system of a surface vessel needs to be designed for improving performance, efficiency, and robustness.

The motion of a ship can be defined in six degrees of freedom (DOFs) and denoted by six differential equations.[2] A historical evolution of these equations is explained by Clarke.[3] Using Froude's scaling law, the designs of autopilot systems using these equations can be tested on scale replica models of actual ocean vessels.[4] Therefore, the mathematical models of these replicas are of great interest, and some of them can be found in the studies by Kang et al.[5] and Skjetne et al.[6] Based on these models, an effective and efficient control scheme should be designed for actual ships.

The traditional autopilot system usually uses a proportional–derivative (PD) controller, which has constant parameters for proportional and derivative coefficients. But the quality of PD control is deteriorated when there are changes in speed, weight, and so on, of the ship or there are external disturbances. Therefore, there is a need for designing a robust control system that means a control system in which the quality of control doesn't degrade even if some parameters of the ship change.[7] In order to solve this problem, various control strategies like adaptive control,[6,8–11] adaptive fuzzy logic control,[12,13] neural network control,[14] adaptive neural control,[15–17] neural dynamic surface

College of Automation Engineering, Nanjing University of Aeronautics and Astronautics, Nanjing, China

Corresponding author:
Mou Chen, College of Automation Engineering, Nanjing University of Aeronautics and Astronautics, 29 Jiangjun Avenue, Jiangning District, Nanjing 211106, Jiangsu Province, P. R. China.
Email: chenmou@nuaa.edu.cn

control,[18,19] fuzzy PID control,[20] sliding mode control (SMC),[7,21,22] and so on, have been proposed.

Among the various robust control strategies, SMC had been mostly studied due to its simplicity, good transient response, robustness, quick response, suppression of external bounded disturbances, and independency of the system dynamics.[23] The idea of SMC had been first published by Itkis[24] and Vadim.[25] This type of control, which is a special type of variable structure control, consists of two parts, a linear or equivalent part and a discontinuous or switching part. The switching part makes the system robust for matched uncertainty.[7] A detailed survey had been discussed in the study by Hung et al.[26] In the study by Tomera,[7] a sliding mode controller was found to have better control action and a lower cost function as compared with a PD controller for a model ship named "Cybership II". An experimental analysis of SMC had been done in the study by Tannuri et al.[27] for a reduced scale model of an off-loading tanker ship. While in the study by Shi,[21] SMC had been designed for the autopilot system of an autonomous underwater vehicle (AUV) in order to eliminate the steady-state error. Afterward, it had been simulated using the mathematical model of an AUV named remote environmental monitoring units for steering, diving, and speed controlling in the presence of disturbance due to waves. A novel fuzzy SMC named fuzzy variable structure SMC had been designed and simulated for a huge ship in order to suppress chattering for its heading control.[28] In this article, chattering is an undesirable phenomenon which is discussed in the end of "Design of sliding mode control with input saturation" section. However, the input saturation needs to be further considered in designing a SMC scheme for a ship.

The input of any real-world system is limited in magnitude and it is called saturation. Input saturation degrades the quality of the control and can even destabilize the system. Therefore, prior to design any control scheme, it is necessary to consider the input constraint. To overcome this, two different methods were explained in the study by Fulwani and Bandyopadhyay,[29] a time-varying sliding surface was designed in the study by Corradini and Orlando,[30] optimal sliding surface was designed in the study by Bartoszewicz and Nowacka-Leverton,[31] and a second-order sliding mode was used in the study by Ferrara and Rubagotti.[32] In the study by Torchani et al.,[33] sliding mode controller was designed for uncertain saturated systems with root clustering in linear matrix inequality region. Other techniques to tackle input saturation are auxiliary system,[34] dynamic surface control,[35] and adaptive fuzzy control.[36,37] However, a little study has been done in this field for vessels and more research is required. The main purpose of this article is to design an efficient, chattering-free steering autopilot system in the presence of actuator saturation.

The remainder of this article is organized as follows. In "Mathematical model of a ship" section, the modeling of a ship is discussed, followed by discussion of the SMC design for saturated systems in "Sliding mode control design" section. "Simulation results" section investigates the simulation results for the proposed scheme followed by a conclusion in the last section.

Notation: $\dot{x}$ and $\ddot{x}$ denote the first and second time derivatives of $x(t)$, respectively. $|.|$ denotes the absolute value unless specified. $\mathrm{sgn}(.)$ and $\mathrm{sat}(.)$ denote the sign and saturation functions, respectively.

Mathematical model of a ship

Kinematics

The marine vessels which operate in a local area and have almost constant latitude and longitude, an earth-fixed frame called the north east down coordinate system referred as n-frame, can be used for its navigation. This navigation is usually called flat earth navigation because it is considered inertial and Newton's laws still apply. It is usually defined as x-axis pointing toward true north, the y-axis toward east, and the z-axis downward normal to the earth's surface. Another moving frame is attached to the vessel, which is fixed to the vessel and it is called body-fixed coordinate system referred here as b-frame. These concepts can be more clearly understood by Figure 1. Hence, the linear and angular velocities should be expressed in the b-frame and the position (x, y) in the n-frame.[2]

Dynamics

The motion of a marine vessel classified in six DOFs, defined according to the Society of Naval Architects and Marine Engineers (SNAME)[1] notation (1950), is shown in Table 1. Moreover, its motion can be described by the following vectors[38]

$$\eta = \begin{bmatrix} \eta_1 \\ \eta_2 \end{bmatrix}, \eta_1 = \begin{bmatrix} x \\ y \\ z \end{bmatrix}, \eta_2 = \begin{bmatrix} \phi \\ \theta \\ \psi \end{bmatrix}, \nu = \begin{bmatrix} \nu_1 \\ \nu_2 \end{bmatrix}, \nu_1 = \begin{bmatrix} u \\ v \\ w \end{bmatrix}, \nu_2 = \begin{bmatrix} p \\ q \\ r \end{bmatrix},$$

$$\tau = \begin{bmatrix} \tau_1 \\ \tau_2 \end{bmatrix}, \tau_1 = \begin{bmatrix} X \\ Y \\ Z \end{bmatrix}, \tau_2 = \begin{bmatrix} K \\ M \\ N \end{bmatrix}$$

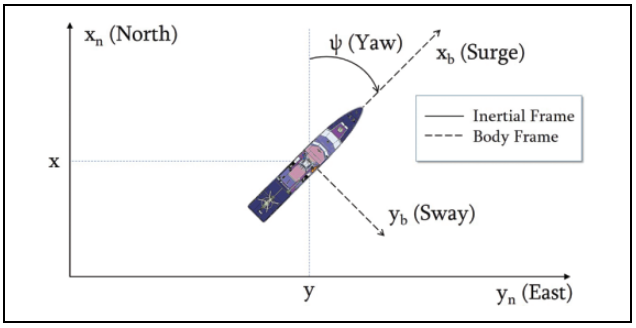

Figure 1. Inertial NED frame and body-fixed frame for a ship with heading angle ψ. NED: north east down.

Table 1. Notation used for vessels.[38]

DOF	Motion/rotation	Force/ moment (units)	Linear/ angular velocity (units)	Displacement/ angle (units)
1	In *x*-direction (surge)	$\mathcal{X}$ (N)	*u* (m/s)	*x* (m)
2	In *y*-direction (sway)	$\mathcal{Y}$ (N)	*v* (m/s)	*y* (m)
3	In *z*-direction (heave)	$\mathcal{Z}$ (N)	*w* (m/s)	*z* (m)
4	About *x*-axis (roll)	$\mathcal{K}$ (Nm)	*p* (rad/s)	ϕ (rad)
5	About *y*-axis (pitch)	$\mathcal{M}$ (Nm)	*q* (rad/s)	θ (rad)
6	About *z*-axis (yaw)	$\mathcal{N}$ (Nm)	*r* (rad/s)	ψ (rad)

DOF: degree of freedom.

where η_1 and η_2 denote the position and orientation vectors, respectively, and η denotes the position and orientation vector defined in the n-frame. Similarly, ν_1 and ν_2 denote the linear and angular velocities, respectively, and ν denotes the linear and angular velocity vectors according to b-frame. τ_1 and τ_2 represent the forces and moments, respectively, while τ is used to indicate the forces and moments acting on the vessel in b-frame. To design the SMC scheme for a ship, the following assumption is needed.

Assumption 1. We assume that the ship is stable in the surge and sway directions and they have negligible amplitudes $\phi \approx \theta \approx \dot{\phi} \approx \dot{\theta} \approx 0$. Similarly, we can also assume the ship is sailing on the water surface with $z \approx 0$ on the average.[2,39]

According to Assumption 1, we can neglect roll, pitch, and heave dynamics. Therefore, the kinematic equations of motion reduce from six DOFs to three DOFs and now the state vectors are $\eta = [x, y, \psi]^T$ and $\nu = [u, v, r]^T$.

The n-frame velocity vector is related to the b-frame velocity vector with one principal rotation about the *z*-axis according to the following kinematic relation[7]

$$\dot{\eta} = R(\psi)\nu \tag{1}$$

where $R(\psi)$ is the rotation matrix defined as[7]

$$R(\psi) = \begin{bmatrix} \cos(\psi) & -\sin(\psi) & 0 \\ \sin(\psi) & \cos(\psi) & 0 \\ 0 & 0 & 1 \end{bmatrix} \tag{2}$$

Rigid-body dynamics

By Newton's second law of motion, the rigid-body equation of motion can be written as[2]

$$M_{RB}\dot{\nu} + C_{RB}(\nu)\nu = \tau_{RB} \tag{3}$$

where M_{RB} is the rigid-body system inertia matrix, $C_{RB}(\nu)$ is the corresponding centripetal and Coriolis matrix, and τ_{RB} is a generalized vector of external forces and moments. For the matrices, M_{RB} and $C_{RB}(\nu)$, we give the following assumption.

Assumption 2. Let the ship be port-starboard symmetric (*xz*-plane symmetry) having homogeneous mass distribution and the center of gravity located at a distance x_g along the body *x*-axis of the b-frame and $y_g = 0$.[2]

Considering Assumption 2, M_{RB} can be written as

$$M_{RB} = \begin{bmatrix} m & 0 & 0 \\ 0 & m & mx_g \\ 0 & mx_g & I_z \end{bmatrix}$$

where m is the mass of the ship and I_z is the moment of inertia about *z*-axis in the b-frame. The Coriolis–centripetal matrix $C_{RB}(\nu)$ can be written skew-symmetrically as

$$C_{RB}(\nu) = \begin{bmatrix} 0 & 0 & -m(x_g r + v) \\ 0 & 0 & mu \\ m(x_g r + v) & -mu & 0 \end{bmatrix}$$

Hydrodynamics

In an ideal fluid, there are several hydrodynamic effects such as added mass, restoring forces, and radiation-induced potential damping. Moreover, there are other damping effects including skin friction, wave drift damping, and vortex shedding. In the current simplified scenario of three DOFs model, the minor effects can be neglected.[6] Considering the major hydrodynamic effects, equation (3) can now be written as[2]

$$M\dot{\nu} + C(\nu)\nu + D(\nu)\nu = \tau \tag{4}$$

where $M = M_{RB} + M_A$, $C(\nu) = C_{RB}(\nu) + C_A(\nu)$, and $D(\nu) = D_L + D_{NL}(\nu)$. And we have

$$M_A = \begin{bmatrix} -X_{\dot{u}} & 0 & 0 \\ 0 & -Y_{\dot{v}} & -Y_{\dot{r}} \\ 0 & -N_{\dot{v}} & -N_{\dot{r}} \end{bmatrix} \text{ and}$$

$$C_A(\nu) = \begin{bmatrix} 0 & 0 & c_{13}(\nu) \\ 0 & 0 & -c_{23}(\nu) \\ -c_{13}(\nu) & c_{23}(\nu) & 0 \end{bmatrix}$$

where $c_{13}(\nu) = Y_{\dot{v}}v + (Y_{\dot{r}} + N_{\dot{v}})r/2$ and $c_{23}(\nu) = X\dot{u}u$ and

$$D_L = \begin{bmatrix} -X_u & 0 & 0 \\ 0 & -Y_v & -Y_r \\ 0 & -N_v & -N_r \end{bmatrix} \text{ and } D_{NL}(\nu) = -\begin{bmatrix} X_{|u|u}|u| + X_{uuu}u^2 & 0 & 0 \\ 0 & Y_{|v|v}|v| + Y_{|r|v}|r| & Y_{|v|r}|v| + Y_{|r|r}|r| \\ 0 & N_{|v|v}|v| + N_{|r|v}|r| & N_{|v|r}|v| + N_{|r|r}|r| \end{bmatrix}$$

where $X_{(.)}$, $Y_{(.)}$, and $N_{(.)}$ are the hydrodynamic parameters according to the notation of SNAME.[8] For low-speed applications, it is convenient to neglect the nonlinear damping matrix and replace $N_{\dot{v}}$ with $Y_{\dot{r}}$.[2] Thus, we have

$$D(\nu) \approx D_L, c_{13}(\nu) = Y_{\dot{v}}v + Y_{\dot{r}}r \tag{5}$$

Model decoupling

The mathematical model discussed in the previous section, represented by equation (4), can be simplified by supposing a constant surge speed $u = u_0$. The sway–yaw dynamics can be separated from the surge model assuming port-starboard symmetry. This sway–yaw model can be written as[2]

$$M_{YN}\dot{\nu}_{YN} + N(u_0)\nu_{YN} = \tau_{YN} \tag{6}$$

where $\nu_{YN} = [v, r]^T$ is the state vector, τ_{YN} is a vector which represents the force and moment in sway and yaw directions, respectively, and

$$M_{YN} = \begin{bmatrix} m - Y_{\dot{v}} & mx_g - Y_{\dot{r}} \\ mx_g - Y_{\dot{r}} & I_z - N_{\dot{r}} \end{bmatrix} \tag{7}$$

$$N(u_0) = \begin{bmatrix} -Y_v & -Y_r + (m - X_{\dot{u}})u_0 \\ -N_v + (X_{\dot{u}} - Y_{\dot{v}})u_0 & -N_r + (mx_g - Y_{\dot{r}})u_0 \end{bmatrix} \tag{8}$$

Here, $N(u_0)$ can be obtained by the summation of the Coriolis–centripetal matrix $C_{YN}(u_0)$ and the linear damping D_{LYN}, that is[2]

$$N(u_0) = C_{YN}(u_0) + D_{LYN} \tag{9}$$

where

$$C_{YN}(u_0) = \begin{bmatrix} 0 & (m - X_{\dot{u}})u_0 \\ (X_{\dot{u}} - Y_{\dot{v}})u_0 & (mx_g - Y_{\dot{r}})u_0 \end{bmatrix},$$
$$D_{LYN} = \begin{bmatrix} -Y_v & -Y_r \\ -N_v & -N_r \end{bmatrix} \tag{10}$$

If the ship is controlled by a single rudder, then we obtain

$$\tau_{YN} = b\delta \tag{11}$$

where

$$b = \begin{bmatrix} -Y_\delta \\ -N_\delta \end{bmatrix} \tag{12}$$

where Y_δ and N_δ are the coefficients of force in sway and moment in yaw, respectively.[2]

The model in equation (6) is linear, and it can be written in the form of Davidson and Schiff.[2,40] Now, this model can be transformed into Nomoto's model by eliminating the sway velocity written as[2,41]

$$\frac{r(s)}{\delta(s)} = \frac{K(1 + T_3 s)}{(1 + T_1 s)(1 + T_2 s)} \tag{13}$$

The above transfer function is called Nomoto's transfer function, and time constants $T_i, (i = 1, 2, 3)$ and the gain constant K are related to the hydrodynamic coefficients according to the following equations[7]

$$T_1 T_2 = \frac{|M|}{|N|} \tag{14}$$

$$T_1 + T_2 = \frac{n_{11}m_{22} + n_{22}m_{11} - n_{12}m_{21} - n_{21}m_{12}}{|N|} \tag{15}$$

$$K = \frac{n_{11}b_2 - n_{21}b_1}{|N|} \tag{16}$$

$$T_3 = \frac{m_{11}b_2 - m_{21}b_1}{K|N|} \tag{17}$$

where the coefficients m_{ij}, n_{ij}, and b_i are the components of the matrices M, N, and b in equation (6), and $|M|$ and $|N|$ are the determinants of the matrices M and N, respectively. Here, an assumption is made as follows:

Assumption 3. For the above Nomoto's model in equation (13), it is assumed that a positive deflection δ will give a positive yaw rate r and vice versa.

According to Assumption 3, the value of K cannot be negative. Experimentally, the time constants T_2 and T_3 are found to be nearly equal.[42] Hence, the order of equation (13) can be reduced by introducing an effective time constant $T = T_1 + T_2 - T_3$, thus we get

$$\frac{r(s)}{\delta(s)} = \frac{K}{1 + Ts} \tag{18}$$

From Figure 2, which illustrates the stern of a ship, it can be inferred that $-U_m \le \delta \le U_m$ or $|\delta| \le U_m$, where U_m is the maximum rudder deflection. By using final value theorem for equation (18), the maximum yaw rate can be calculated as

$$r_m = KU_m \tag{19}$$

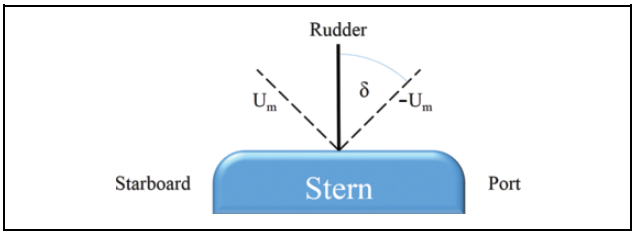

Figure 2. The maximum rudder deflection on both sides.

where r_m is named as the maximum yaw rate. By Assumption 3, equation (19) can be split as

$$r_{m-} = -KU_m \quad \text{in port direction} \tag{20}$$

$$r_{m+} = KU_m\,, \text{ in starboard direction} \tag{21}$$

Considering Assumption 1, we get $r = \dot{\psi}$. Finally, the Nomoto's first-order and second-order models, respectively, in equations (18) and (13) can be written in the form of ψ as

$$\frac{\psi(s)}{\delta(s)} = \frac{K(1+T_3 s)}{s(1+T_1 s)(1+T_2 s)} \approx \frac{K}{s(1+Ts)} \tag{22}$$

Due to the simplicity and effectiveness of the above model, it is commonly used for steering in autopilot systems.[7,38] Moreover, it can be written in the form of a state equation considering input saturation as[7]

$$\begin{bmatrix} \dot{\psi} \\ \dot{r} \end{bmatrix} = \begin{bmatrix} 0 & 1 \\ 0 & a \end{bmatrix} \begin{bmatrix} \psi \\ r \end{bmatrix} + \begin{bmatrix} 0 \\ b \end{bmatrix} \text{sat}\,(\delta) \tag{23}$$

where

$$r = \frac{d\psi}{dt}, a = -\frac{1}{T}, b = \frac{K}{T} \tag{24}$$

and

$$\text{sat}\,(\delta) = \begin{cases} U_m, & \text{if} \quad \delta > U_m \\ \delta, & \text{if} \quad -U_m \le \delta \le U_m \\ -U_m, & \text{if} \quad \delta < -U_m \end{cases} \tag{25}$$

Model of Esso Osaka tanker

The real "Esso Osaka" tanker was scaled down by 1:100 ($k = 100$) to create a model, which is used for experimentation and verification of various control and guidance systems. The physical model of this ship is present in the Marine Cybernetics Laboratory, Department of Engineering Cybernetics, Norwegian University of Science and Technology, Trondheim, Norway. The main characteristics of this ship are listed in Table 2.

For this ship moving at a speed of 0.4 m/s, the values of K and T of the equation (18) are calculated as 0.1705 s^{-1} and 7.1167 s, respectively.[38] After transforming this into equation (23), we can find the values of a and b as -0.1405 and 0.0240, respectively.

Table 2. "Esso Osaka" model particulars.[38]

Particulars	Symbol	Values
Length	L	3.430 m
Length between perpendiculars	L_{pp}	3.250 m
Breadth	B	0.530 m
Draft (estimated at trials)	D	0.217 m
Number of rudders	R	1
Displacement (estimated at trials)	W	319.40 kg
Rudder area	R_A	0.0120 m^2
Propeller area	P_A	0.0065 m^2
Longitudinal CG (forward of midship)	x_g	0.103 m

CG: center of gravity.

Sliding mode control design

Design of sliding mode control with input saturation

Sliding mode controller is a robust controller in which matched uncertainty doesn't deteriorate the control quality. The structure of the sliding mode controller usually consists of two parts, linear control and nonlinear control. The linear control is called equivalent part, which is designed for linearized system and is responsible to control while the system is on the sliding mode surface. The second part is a switching controller, which is responsible to take the system to the sliding mode surface. While on sliding mode surface, the system becomes insensitive to external disturbances and parametric variations to some extent.[27] Its structure can be represented as

$$u = u_{eq} + u_{sw} \tag{26}$$

where u_{eq} is the linear part and u_{sw} is the non linear part of the controller. To design the controller, the system defined in equation (23) can be written as

$$\dot{x} = Ax + Bu_s \tag{27}$$

where

$$A = \begin{bmatrix} 0 & 1 \\ 0 & a \end{bmatrix}, x = \begin{bmatrix} x_1 \\ x_2 \end{bmatrix} = \begin{bmatrix} \psi \\ r \end{bmatrix}, B = \begin{bmatrix} 0 \\ b \end{bmatrix},$$
$$u_s = \text{sat}(u) = \text{sat}(\delta) \tag{28}$$

The sliding mode surface is designed as

$$\sigma = Se \tag{29}$$

where $e = x - x_r$ and $x_r = \begin{bmatrix} x_{1r} \\ x_{2r} \end{bmatrix} = \begin{bmatrix} \psi_r \\ r_r \end{bmatrix}$ is the vector consisting of commanded heading and yaw rate, respectively, and

$$S = [\,S_1 \quad S_2\,] \tag{30}$$

where $S_1 > 0$ and $S_2 > 0$ are the design constants and should make SB nonsingular. Substituting equation (30) into equation (29) yields

$$\sigma = S_1 e_1 + S_2 e_2 \tag{31}$$

where $e_1 = x_1 - x_{1r}$ and $e_2 = x_2 - x_{2r}$. By taking derivative on both sides of equation (29) gives

$$\dot{\sigma} = S\dot{e} = S(\dot{x} - \dot{x}_r) \tag{32}$$

where $\dot{e} = \dot{x} - \dot{x}_r$. To avoid the saturation, we need to consider $u = u_s$ and by substituting from equation (27) into the last equation, it can be expressed as

$$\dot{\sigma} = S(Ax + Bu - \dot{x}_r) = SAx + SBu - S\dot{x}_r \tag{33}$$

By taking $\dot{\sigma} = 0$, the equivalent control can be found as

$$u_{eq} = (SB)^{-1} S(\dot{x}_r - Ax) \tag{34}$$

The switching control can be designed as

$$u_{sw} = -(SB)^{-1} \rho \,\mathrm{sgn}(\sigma) \tag{35}$$

where ρ is to be designed to select the gain of the switching part and it should not be confused with the position and orientation vector described in "Mathematical model of a ship" section. The value of ρ determines how quickly the system will reach the sliding mode surface.[43] Moreover, $\mathrm{sgn}(.)$ is the sign function defined as

$$\mathrm{sgn}(\sigma) = \begin{cases} 1, & \text{if} \quad \sigma > 0 \\ 0, & \text{if} \quad \sigma = 0 \\ -1, & \text{if} \quad \sigma < 0 \end{cases} \tag{36}$$

Then, the sliding mode control scheme can be written as

$$u = (SB)^{-1}[S(\dot{x}_r - Ax) - \rho \,\mathrm{sgn}(\sigma)] \tag{37}$$

Invoking the definitions of all variables yields

$$u = (S_2 b)^{-1}[S_1(\dot{x}_{1r} - x_2) + S_2(\dot{x}_{2r} - a x_2) - \rho \,\mathrm{sgn}(\sigma)] \tag{38}$$

To avoid any nonlinearity or instability, the actuator should not reach saturation limitation. Hence, it should be guaranteed that

$$|u| < U_m \tag{39}$$

or

$$-U_m < u < U_m \tag{40}$$

The rudder deflection on both sides can be treated separately; therefore, the last inequality can be split as

$$u > -U_m \tag{41}$$

$$u < U_m \tag{42}$$

Before substituting the control output in inequalities (41) and (42), we know from equation (38) the value of sign function $\mathrm{sgn}(.)$ depends upon σ. Moreover, it should be noted that when $\mathrm{sgn}(\sigma) = 0$, then the system is in sliding mode and there is no need to evaluate ρ in this case. Thus, there are two possibilities left with respect to $\mathrm{sgn}(\sigma)$ as follows:

Case A: $\sigma < 0, \mathrm{sgn}(\sigma) = -1$. By substituting value of u from equation (38) into the last two inequalities (41) and (42) and then substituting r_{m-} and r_{m+} for negative and positive yaw rate, respectively, in place of x_2, we obtain

$$\frac{1}{S_2 b}[S_1(\dot{x}_{1r} - r_{m-}) + S_2(\dot{x}_{2r} - a r_{m-}) + \rho] > -U_m \tag{43}$$

$$\frac{1}{S_2 b}[S_1(\dot{x}_{1r} - r_{m+}) + S_2(\dot{x}_{2r} - a r_{m+}) + \rho] < U_m \tag{44}$$

Substituting the respective maximum possible yaw rate from equations (20) and (21) into the last two inequalities yields

$$\frac{1}{S_2 b}[S_1(\dot{x}_{1r} + KU_m) + S_2(\dot{x}_{2r} + aKU_m) + \rho] > -U_m \tag{45}$$

$$\frac{1}{S_2 b}[S_1(\dot{x}_{1r} - KU_m) + S_2(\dot{x}_{2r} - aKU_m) + \rho] < U_m \tag{46}$$

From equation (24), the value of K can be found as[7]

$$K = -\frac{b}{a} \tag{47}$$

Considering equations (45), (46), and (47), these can be written as

$$\frac{1}{S_2 b}\left[S_1\left(\dot{x}_{1r} - \frac{bU_m}{a}\right) + S_2(\dot{x}_{2r} - bU_m) + \rho\right] > -U_m \tag{48}$$

$$\frac{1}{S_2 b}\left[S_1\left(\dot{x}_{1r} + \frac{bU_m}{a}\right) + S_2(\dot{x}_{2r} + bU_m) + \rho\right] < U_m \tag{49}$$

Finally, the value of ρ for this case can be found as

$$-\begin{bmatrix} S_1 & S_2 \end{bmatrix}\begin{bmatrix} \dot{x}_{1r} + KU_m \\ \dot{x}_{2r} \end{bmatrix} < \rho < -\begin{bmatrix} S_1 & S_2 \end{bmatrix}\begin{bmatrix} \dot{x}_{1r} - KU_m \\ \dot{x}_{2r} \end{bmatrix} \tag{50}$$

The above inequality can be used to choose the value of η to avoid saturation for $\mathrm{sgn}(\sigma) = -1$.

Case B: $\sigma > 0, \mathrm{sgn}(\sigma) = 1$. Similarly, by substituting value of u into inequalities (41) and (42) and afterwards substituting r_{m-} and r_{m+} for x_2, we obtain

$$\frac{1}{S_2 b}[S_1(\dot{x}_{1r} - r_{m-}) + S_2(\dot{x}_{2r} - a r_{m-}) - \rho] > -U_m \tag{51}$$

$$\frac{1}{S_2 b}[S_1(\dot{x}_{1r} - r_{m+}) + S_2(\dot{x}_{2r} - a r_{m+}) - \rho] < U_m \tag{52}$$

and substituting the respective maximum possible yaw rate from equations (20) and (21) to the above inequalities yields

$$\frac{1}{S_2 b}[S_1(\dot{x}_{1r} + KU_m) + S_2(\dot{x}_{2r} + aKU_m) - \rho] > -U_m \tag{53}$$

$$\frac{1}{S_2 b}[S_1(\dot{x}_{1r} - KU_m) + S_2(\dot{x}_{2r} - aKU_m) - \rho] < U_m \tag{54}$$

Considering equations (53), (54), and (47), these can be written as

$$\frac{1}{S_2 b}\left[S_1\left(\dot{x}_{1r}-\frac{bU_m}{a}\right)+S_2(\dot{x}_{2r}-bU_m)-\rho\right]>-U_m \tag{55}$$

$$\frac{1}{S_2 b}\left[S_1\left(\dot{x}_{1r}+\frac{bU_m}{a}\right)+S_2(\dot{x}_{2r}+bU_m)-\rho\right]<U_m \tag{56}$$

Similarly, for this case, the value of ρ can be found as

$$[S_1 \quad S_2]\begin{bmatrix}\dot{x}_{1r}-KU_m\\ \dot{x}_{2r}\end{bmatrix}<\rho<[S_1 \quad S_2]\begin{bmatrix}\dot{x}_{1r}+KU_m\\ \dot{x}_{2r}\end{bmatrix} \tag{57}$$

The above inequality can be used to choose the value of ρ to avoid saturation for $\mathrm{sgn}(\sigma)=1$.

In the proposed algorithm, the values of K, S_1, S_2, ρ, and U_m are positive. If σ is positive, then case A should be satisfied, and if σ is negative, then case B should be satisfied. Based upon the above analysis, the following theorem can be summarized.

Theorem 1. A steering system of a ship is considered with input saturation. All states are available and the sliding mode control scheme is designed as equation (38). Then, all signals of the close-loop system are convergent, if the value of ρ is positive and satisfies (65).

Proof. According to Lyapunov stability theorem, the origin of a system is asymptotically stable, if there is a positive definite function V, such that $\dot{V}$ is negative definite.[44] Thus, let us consider a Lyapunov function as

$$V=\frac{1}{2}\sigma^2 \tag{58}$$

By substituting values from equation (29), we have

$$V=\frac{1}{2}(S_1e_1+S_2e_2)^2 \tag{59}$$

It can be stated that the above function is positive. Taking derivative yields

$$\begin{aligned}\dot{V}&=S_1^2e_1\dot{e}_1+S_2^2e_2\dot{e}_2+S_1S_2\dot{e}_1e_2+S_1S_2e_1\dot{e}_2\\&=(S_1\dot{e}_1+S_2\dot{e}_2)(S_1e_1+S_2e_2)\\&=\dot{\sigma}\sigma\end{aligned} \tag{60}$$

Now substituting the value of $\dot{\sigma}$ into the above equation from equation (33) yields

$$\dot{V}=(SAx+SBu-S\dot{x}_r)\sigma \tag{61}$$

Substituting the value of u from equation (38) gives

$$\begin{aligned}\dot{V}&=SAx\sigma+[S\dot{x}_r-SAx-\rho\,\mathrm{sgn}(\sigma)]\sigma-S\dot{x}_r\sigma\\&=-\rho\,\mathrm{sgn}(\sigma)\sigma\end{aligned} \tag{62}$$

From the definition of signum (or sign) function, we know that $|\sigma|=\mathrm{sgn}(\sigma)\sigma$. Thus, equation (62) can be written as

$$\dot{V}=-\rho|\sigma| \tag{63}$$

The value of the last equation will be negative, only if ρ is positive, that is

$$\rho>0 \tag{64}$$

which is the condition for the stability of the system and the proof is concluded. A criteria for selection of η can be written in a nutshell as

$$\rho=\begin{cases}-[S_1 \quad S_2]\begin{bmatrix}\dot{x}_{1r}+KU_m\\ \dot{x}_{2r}\end{bmatrix}<\rho<-[S_1 \quad S_2]\begin{bmatrix}\dot{x}_{1r}-KU_m\\ \dot{x}_{2r}\end{bmatrix} & \text{and, } \rho>0, \text{ if } \sigma<0\\ [S_1 \quad S_2]\begin{bmatrix}\dot{x}_{1r}-KU_m\\ \dot{x}_{2r}\end{bmatrix}<\rho<[S_1 \quad S_2]\begin{bmatrix}\dot{x}_{1r}+KU_m\\ \dot{x}_{2r}\end{bmatrix} & \text{and, } \rho>0, \text{ if } \sigma>0\end{cases} \tag{65}$$

Remark 1. To maintain any fixed value of the output of the ship using control techniques is called set point regulation. In this case, the direction of the ship (i.e. ψ) can be regulated by keeping $\dot{x}_{1r}$ and $\dot{x}_{2r}$ equal to zero in *Case A* or *Case B*, which yields

$$-S_1KU_m<\rho<S_1KU_m \text{ and } \eta>0 \tag{66}$$

or

$$0<\rho<S_1KU_m \tag{67}$$

Equation (67) and Theorem 1 can be used for the criteria of set point regulation in the presence of saturation.

Chattering avoidance

A drawback for SMC system is chattering. Chattering is a phenomena of high-frequency oscillations having finite magnitude of the output of the SMC system while operating in the sliding mode surface. In many practical applications, it becomes important to avoid chattering because it can lead to high wear and tear, high temperature, and unwanted excitation of the actuators.[23] For instance, a vessel's hydrodynamic surfaces are not capable of moving with high frequency, but the control system should be effective and in synchronization.[45]

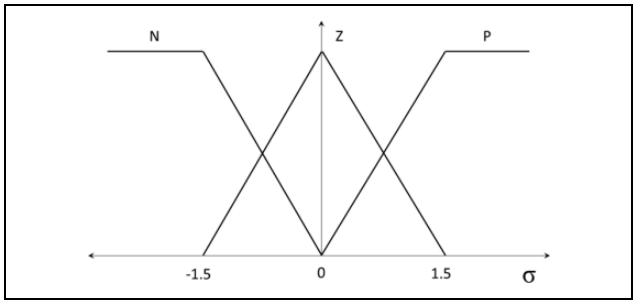

Figure 3. The membership function of fuzzy input σ.

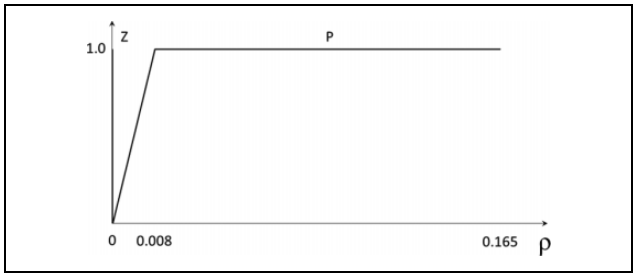

Figure 4. The membership function of fuzzy output ρ.

One method to suppress chattering is using sat(.) (saturation) function instead of the discontinuous sgn(.) function, which can be defined as

$$\text{sat}(\sigma) = \begin{cases} 1, & \text{if} \quad \sigma \geq l \\ \dfrac{\sigma}{l}, & \text{if} \quad -l < \sigma < l \\ -1, & \text{if} \quad \sigma \leq -l \end{cases} \tag{68}$$

where l is any positive number which represents the level of saturation.

However, a better method to suppress chattering is to use fuzzy logic to handle the gain ρ in equation (38). In spite of improving the system performance, using fuzzy SMC, the robustness of the system is also guaranteed.[46] Therefore, the input and output membership functions are designed as shown in Figures 3 and 4, respectively. The rule base of the fuzzy system is designed as[46–48]

If σ is N, then ρ is P
If σ is Z, then ρ is Z
If σ is P, then ρ is P

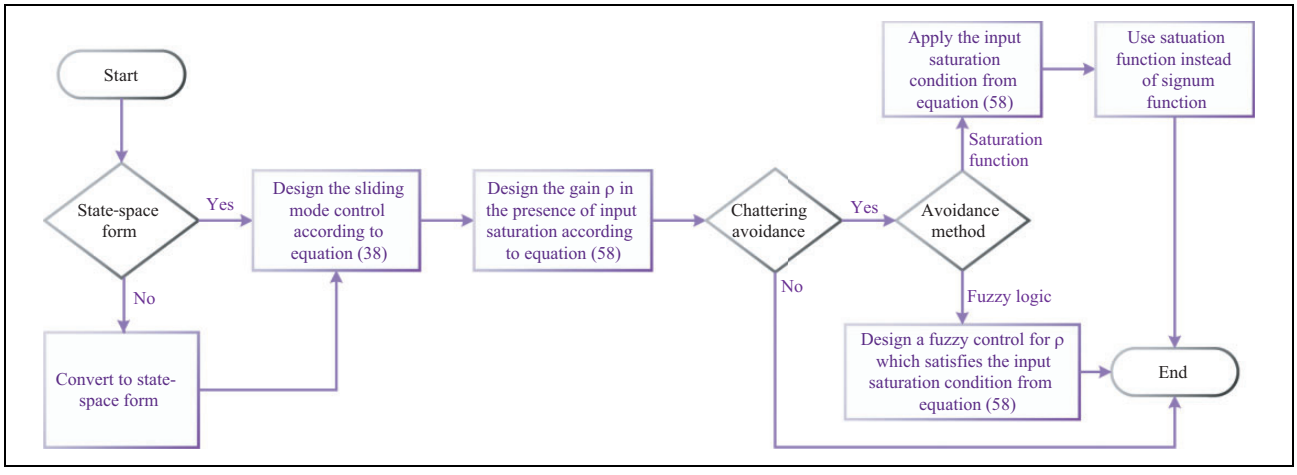

Figure 5. Flowchart of the proposed control system (ψ).

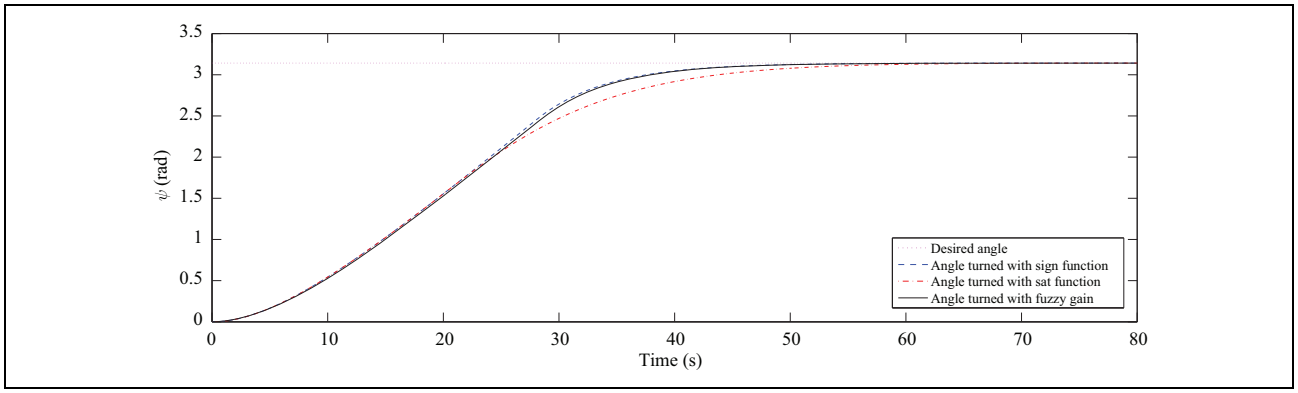

Figure 6. Angle turned by the ship (ψ).

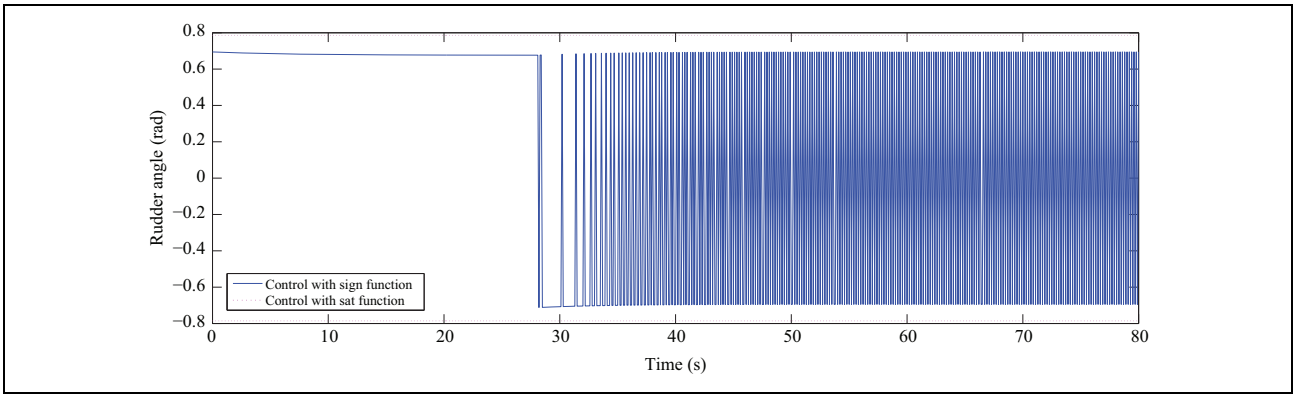

Figure 7. Control output (rudder angle δ).

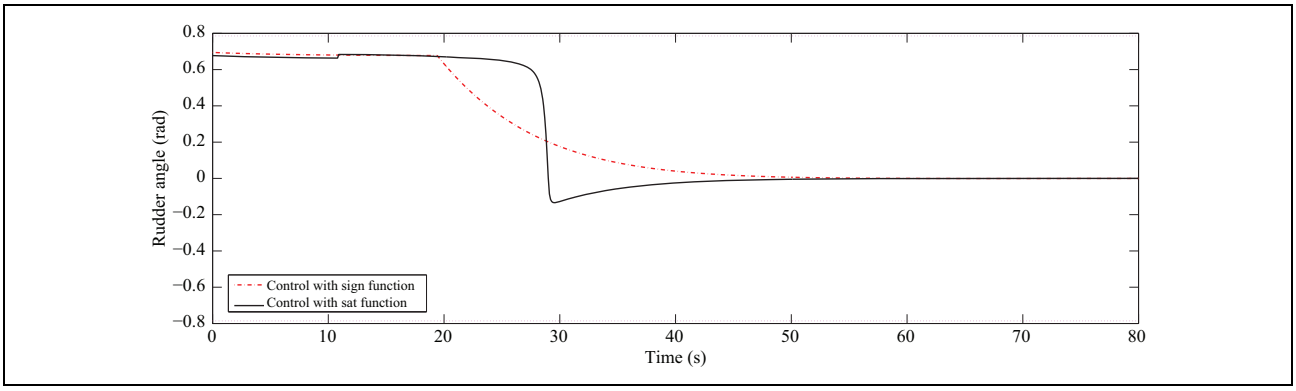

Figure 8. Control output (rudder angle δ).

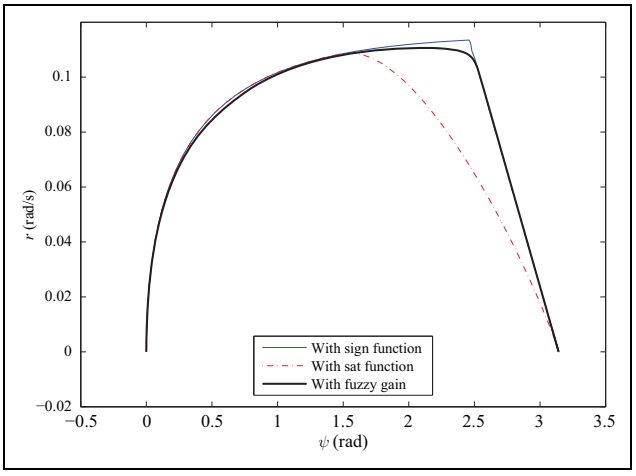

Figure 9. ψ-ψ' plot showing the sliding surface.

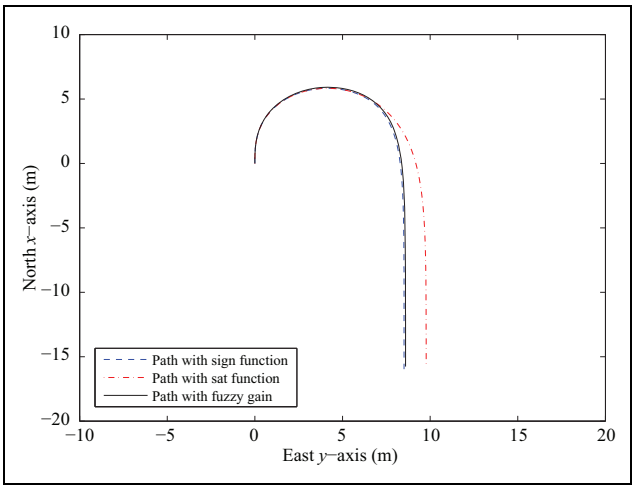

Figure 10. Path followed by the ship.

where N, Z, and P are the fuzzy terms which can be seen from Figures 3 and 4 for fuzzy antecedent and consequent, respectively.

The flowchart for the complete design of the proposed control system is given in Figure 5.

Simulation results

A reduced scale model ship of a tanker named Esso Osaka is simulated assuming calm water with infinite depth. This simulation is performed at the scale of the

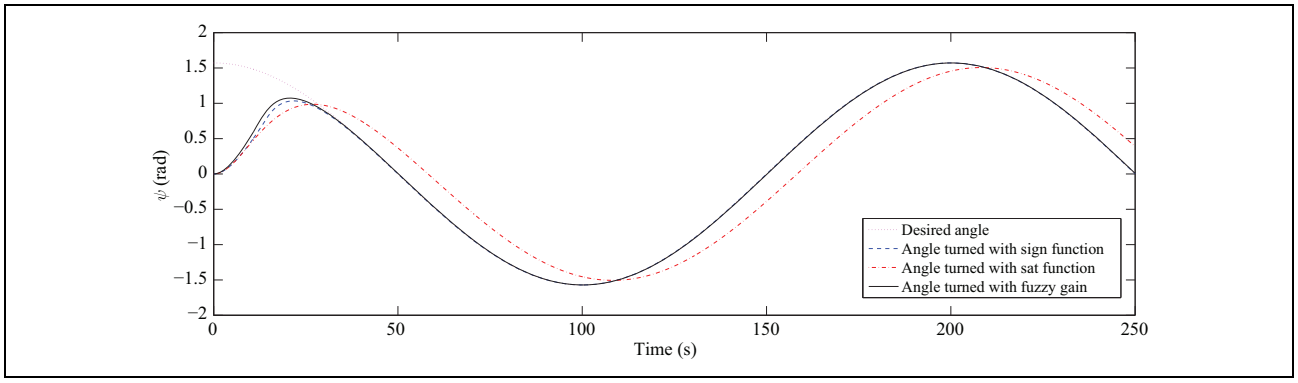

Figure 11. Angle turned by the ship (ψ).

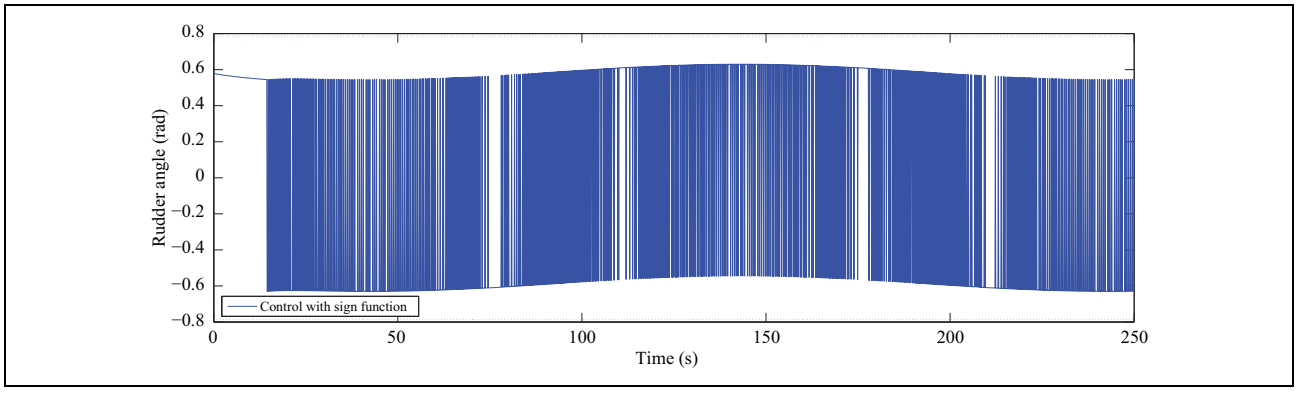

Figure 12. Control output (rudder angle δ).

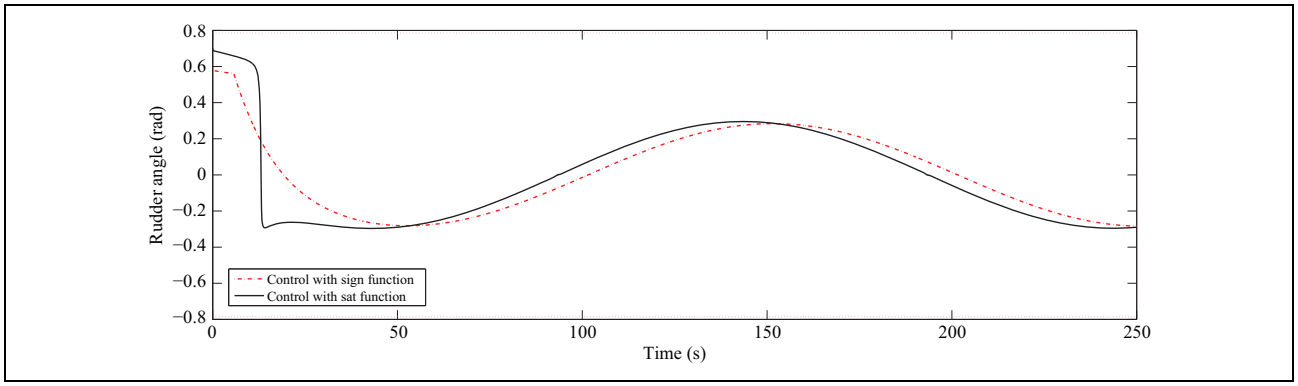

Figure 13. Control output (rudder angle δ).

model ship. It was assumed to move with a constant speed of 0.4 m/s, initially, toward the true north (i.e. x-axis). As assumed in the study by Perera and Soares,[23] the saturation limit of the rudder is considered as $\pi/4$ radians on both sides. The value of l in equation (68) is selected as 1.

The initial conditions can be written as

$$x_1(0) = x_2(0) = 0 \tag{69}$$

Set point regulation

For simulation purpose, a scenario is created, which has an objective that the ship has to turn an angle of 180° ($x_{1r} = \pi$ rad) and regulate this heading ($x_{2r} = 0$). To avoid saturation, equation (67) must be satisfied.

Let us suppose the value of $S_1 = 1$ and $S_2 = 6$, therefore

$$0 < \eta\rho < 0.1339 \tag{70}$$

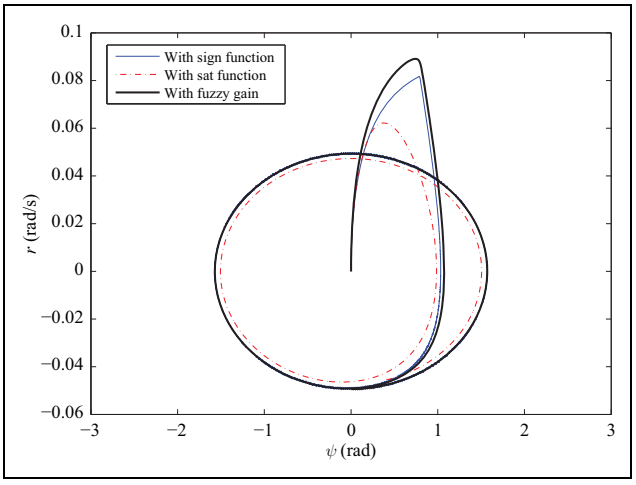

Figure 14. ψ-$\psi^{'}$ plot showing the sliding surface.

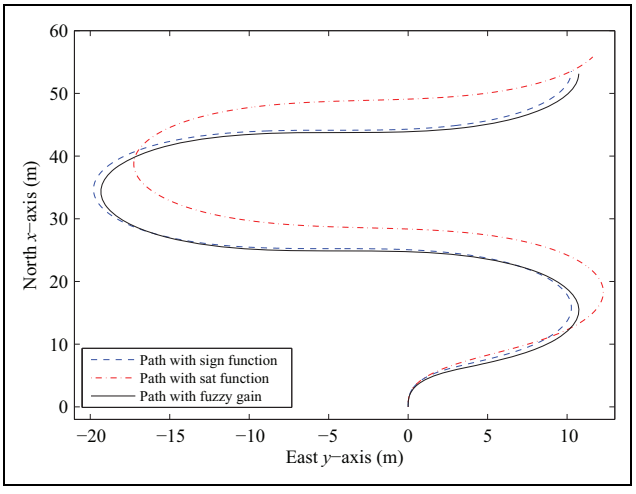

Figure 15. Path followed by the ship.

By fulfilling the above condition, it is ensured that the system will not go in saturation mode. Let the value of $\eta\rho$ be 0.1, which fulfills the above condition. Figure 6 shows the transient response of the system. In this figure, it can be seen that using fuzzy gain for chattering avoidance doesn't deteriorate the results much as compared to using saturation function. The output of the control system, that is, rudder angle, is shown in Figure 7 with sgn(.) function, in which chattering effect can be observed. The output using fuzzy gain and sat(.) functions is shown in Figure 8. The evidence of the sliding mode is shown in Figure 9, in which the sliding surface can be seen for sgn(.) function and fuzzy gain only. The path followed by the ship can be seen from Figure 10, in which it can be seen that it has successfully turned an angle of 180°; however, using the saturation function, the turning radius has increased. Hence, these results conclude that using the traditional sgn(.) function produces chattering effect, which makes the system less efficient. Although the sat(.) function eliminates the chattering, it slows the system and increases the turning radius. Therefore, in this scenario, the proposed method using fuzzy gain is more efficient as compared.

Reference tracking

To further test the control system, we can create a different scenario with the same initial conditions. This time, the ship has to track a cosine wave of frequency equal to $\pi/100 = 0.0314$ rad/s. It can be seen from Figure 11 that initially, the control system attempts to reach the desired angle and after reaching it, it maintains this time-varying signal except for saturation function, in which a delay is also observed. Figures 12 and 13 show the control signals, while Figures 14 and 15 show the $\psi - \psi^{'}$ plot and path followed by the ship, respectively, for this scenario. From these results, we see that although the saturation function eliminates the chattering effect, it produces a delay. This delay makes the control system less efficient, while fuzzy SMC removes the effect of chattering with negligible effect on the system performance.

Conclusion

In this article, SMC has been proposed for the steering control of saturated surface vessels. The autopilot system designed for the mathematical model of the scaled replica of Esso Osaka tanker is simulated in MATLAB to demonstrate the performance of the system. Set point regulation and input tracking are simulated for this scenario. The results show that this controller is effective and stable for saturated actuators and can be readily applied to other vessels. Furthermore, the simulations show that using fuzzy gain for the SMC is much better for chattering avoidance than using saturation function.

Declaration of conflicting interests

The author(s) declared no potential conflicts of interest with respect to the research, authorship, and/or publication of this article.

Funding

The author(s) disclosed receipt of the following financial support for the research, authorship, and/or publication of this article: This work was supported in part by the Fundamental Research Funds for the Central Universities under Grant NE2016101.

References

1. Mackenzie FT. "Hydrosphere". *The Encyclopedia Britannica*.[Internet] The Encyclopedia Britannica, 2005. https://www.britannica.com/science/hydrosphere (Accessed 9 September 2015).
2. Fossen TI. *Marine control systems: guidance, navigation and control of ships, rigs and underwater vehicles*, Trondheim, Norway: Marine Cybernetics, 2002.
3. Clarke D. The foundations of steering and manoeuvring. In: *Proceedings 6th IFAC conference manoeuvering and control marine crafts*, IFAC, Girona, Spain, 17–19 September 2003.

4. Gillmer TC and Johnson B. *Introduction to naval architecture*. Annapolis, Maryland, US: Naval Institute Press, 1982.
5. Kang D, Nagarajan V, Hasegawa K, et al. Mathematical model of single-propeller twin-rudder ship. *J Mar Sci Tech Springer* 2008; 13(3): 207–222.
6. Skjetne R, Smogeli Ø, and Fossen TI. Modeling, identification, and adaptive maneuvering of Cybership II: a complete design with experiments. In: *Proc IFAC conference on control applications in marine systems*, Ancona, Italy, 7–9 July 2004. pp. 203–208.
7. Tomera M. Nonlinear controller design of a ship autopilot. *International Journal of Applied Mathematics and Computer Science* 2010; 20(2): 271–280.
8. Skjetne R, Fossen TI, and Kokotović PV. Adaptive maneuvering, with experiments, for a model ship in a marine control laboratory. *Automatica Elsevier* 2005; 41(2): 289–298.
9. Chen M and Jiang B. Adaptive control and constrained control allocation for overactuated ocean surface vessels. *International Journal of Systems Science* 2013; 44(12): 2295–2309.
10. Chen M, Ge SS, How BV, et al. Robust adaptive position mooring control for marine vessels. *IEEE Transactions on Control Systems Technology* 2013; 21(2): 395–409.
11. Chen M, Jiang B, and Cui RX. Actuator fault-tolerant control of ocean surface vessels with input saturation. *International Journal of Robust and Nonlinear Control. Wiley Online Library* 2016; 26(3): 542–564.
12. Velagic J, Vukic Z, and Omerdic E. Adaptive fuzzy ship autopilot for track-keeping. *Control Engineering Practice* 2003; 11(4): 433–443.
13. Bessa WM, Dutra MS, and Kreuzer E. Depth control of remotely operated underwater vehicles using an adaptive fuzzy sliding mode controller. *Robotics and Autonomous Systems* 2008; 56(8): 670–677.
14. Huang JT. Global tracking control of strict-feedback systems using neural networks. *IEEE Transactions on Neural Networks and Learning Systems* 2012; 23(11): 1714–1725.
15. Pan Y, Liu Y, Xu B, et al. Hybrid feedback feedforward: an efficient design of adaptive neural network control. *IEEE Transactions on Industrial Electronics* 2016; 76: 122–134.
16. Chen M and Ge SS. Adaptive neural output feedback control of uncertain nonlinear systems with unknown hysteresis using disturbance observer. *IEEE Transactions on Industrial Electronics* 2015; 62(12): 7706–7716.
17. Chen M, Shi P, and Lim CC. Adaptive neural fault-tolerant control of a 3-DOF model helicopter system. *IEEE Transactions on Systems, Man, and Cybernetics* 2016; 46(2): 260–270.
18. Xu B, Shi Z, Yang C, et al. Composite neural dynamic surface control of a class of uncertain nonlinear systems in strict-feedback form. *IEEE Transactions on Cybernetics* 2014; 44(12): 2626–2634.
19. Xu B, Yang C, and Pan Y. Global neural dynamic surface tracking control of strict-feedback systems with application to hypersonic flight vehicle. *IEEE Transactions on Neural Networks and Learning Systems* 2015; 26(10): 2563–2575.
20. Polkinghorne MN, Roberts GN, Burns RS, et al. The implementation of fixed rulebase fuzzy logic to the control of small surface ships. *Control Engineering Practice* 1995; 3(3): 321–328.
21. Shi J. Design of sliding mode autopilot with steady-state error elimination for autonomous underwater vehicles. In: *TENCON 2006. IEEE Region 10 conference*, Hong Kong, China, 14–17 November 2006, pp. 1–4.
22. García-Valdovinos LG, Salgado-Jiménez T, Bandala-Sánchez M, et al. Modelling, design and robust control of a remotely operated underwater vehicle. *International Journal of Advanced Robotic Systems* 2014; 11: 1.
23. Perera LP and Soares CG. Pre-filtered sliding mode control for nonlinear ship steering associated with disturbances. *Ocean Engineering Elsevier* 2012; 51: 49–62.
24. Itkis U. *Control systems of variable structure*. New South Wales: Halsted Press, 1976.
25. Vadim IU. Survey paper variable structure systems with sliding modes. *IEEE Transactions on Automatic Control* 1977; 22(2): 212–222.
26. Hung JY, Gao W and Hung JC. Variable structure control: a survey. *IEEE Transactions on Industrial Electronics* 1993; 40(1): 2–22.
27. Tannuri EA, Agostinho AC, Morishita HM, et al. Dynamic positioning systems: an experimental analysis of sliding mode control. *Control Engineering Practice Elsevier* 2010; 18(10): 1121–1132.
28. Liang C and Zhong-Ren L. A study of fuzzy variable structure sliding mode control. In: *IEEE international conference on systems, man, and cybernetics*, Beijing, China, 14–17 October 1996. pp. 372–377.
29. Fulwani D and Bandyopadhyay B. Design of sliding mode controller with actuator saturation. In: *Advances in Sliding Mode Control*. Berlin Heidelberg: Springer, 2013. pp. 207–219.
30. Corradini ML and Orlando G. Linear unstable plants with saturating actuators: robust stabilization by a time varying sliding surface. *Automatica* 2007; 43(1): 88–94.
31. Bartoszewicz A and Nowacka-Leverton A. ITAE optimal sliding modes for third-order systems with input signal and state constraints. *IEEE Transactions on Automatic Control* 2010; 55(8): 1928–1932.
32. Ferrara A and Rubagotti M. A sub-optimal second order sliding mode controller for systems with saturating actuators. *IEEE Transactions on Automatic Control* 2009; 54(5): 1082–1087.
33. Torchani B, Sellami A, and Garcia G. Sliding mode control of class of linear uncertain saturated systems. In: *Advances and Applications in Sliding Mode Control Systems*. Warsaw, Poland: Springer International Publishing, 2015. pp. 137–165.
34. Chen M, Ge SS, and Ren BB. Adaptive tracking control of uncertain MIMO nonlinear systems with input constraints. *Automatica* 2011; 47(3): 452–465.
35. Xu B, Huang XY, Wang DW, et al. Dynamic surface control of constrained hypersonic flight models with parameter

estimation and actuator compensation. *Asian Journal of Control* 2014; 16(1): 162–174.
36. Li Y, Tong S, and Li T. Direct adaptive fuzzy backstepping control of uncertain nonlinear systems in the presence of input saturation. *Neural Computing and Applications* Springer 2013; 23(5): 1207–1216.
37. Li Y, Tong S, and Li T. Adaptive fuzzy output-feedback control for output constrained nonlinear systems in the presence of input saturation. *Fuzzy Sets and Systems* 2014; 248: 138–155.
38. Moreira L, Fossen TI, and Soares CG. Path following control system for a tanker ship model. *Ocean Engineering* 2007; 34(14): 2074–2085.
39. Cheng J, Yi J, and Zhao D. Design of a sliding mode controller for trajectory tracking problem of marine vessels. *IET Control Theory and Applications* 2007; 1(1): 233–237.
40. Davidson KS and Schiff L. Turning and course keeping qualities. *Transactions of Society of Naval Architects and Marine Engineers* 1946; 54(1): 152–200.
41. Nomoto K. On the steering qualities of ships. *International Ship Building Progress* 1957; 4(35): 354–370.
42. Mishra P, Panigrahi SK, and Das S. Ships steering autopilot design by Nomoto model. *International Journal of Mechanical Engineering and Robotics* 2015; 3(3): 37–41.
43. Ashrafiuon H, Muske KR, McNinch LC, et al. Sliding-mode tracking control of surface vessels. *IEEE Transactions on Industrial Electronics* 2008; 55(11): 4004–4012.
44. Levine WS (ed). *The control handbook*. Boca Raton, Florida: CRC press, 1996.
45. Shtessel Y, Edwards C, Fridman L, et al. *Sliding mode control and observation*. Berlin: Springer, 2014.
46. Roopaei M and Jahromi MZ. Chattering-free fuzzy sliding mode control in MIMO uncertain systems. *Nonlinear Analysis* 2009; 71(10): 4430–4437.
47. Liu J and Wang X. Fuzzy sliding mode control. In: *Advanced Sliding Mode Control for Mechanical Systems*. Beijing: Springer Berlin Heidelberg, Tsinghua University Press, 2011. pp. 233–279.
48. Yau HT and Chen CL. Chattering-free fuzzy sliding-mode control strategy for uncertain chaotic systems. *Chaos, Solitons and Fractals* 2006; 30(3): 709–718.